Many-Body Theory of Quantum Noise

C. J. Mertens and T. A. B. Kennedy

School of Physics, Georgia Institute of Technology, Atlanta, Georgia 30332-0430

S. Swain

*Department of Applied Mathematics and Theoretical Physics, The Queen's University of Belfast,
Belfast BT7 1NN, Northern Ireland*

A self-consistent many-body approach to quantum noise is presented. Many-photon polarization effects produce system-size scaling in quantum dissipative systems. The role of system-size quantum noise on the dynamics near the bifurcation point in an optical parametric oscillator is investigated, and nonlinear spectra are presented in the nonadiabatic limit.

The role of thermal noise in nonequilibrium phase transitions, symmetry breaking bifurcations, and nonlinear dynamics is a subject of much interest [1]. More generally quantum noise, the most fundamental noise source, is always present and may be most significant, for example, in dissipative optical systems [2-9]. A fully quantum theoretical treatment of the dynamics is then necessary.

In many quantum optical systems, the radiation field may be considered semiclassical since quantum fluctuations are typically small and perturb the classical Maxwell field only weakly. In cavity quantum electrodynamics [10,11], however, reduced dissipation and resonant coherent couplings produce large quantum fluctuations and intrinsically nonperturbative, quantum dissipative dynamics. This is often very difficult to treat theoretically and general dynamical information in the form of correlation functions, the effects of quantum noise near a bifurcation, and the coherence properties of the output is not readily extracted. The description of such phenomena presents a challenging problem in nonequilibrium quantum statistical physics. Ideally one would like to have a method for the systematic computation of physical observables, such as those measured by photodetection, which also provides insight into the underlying physics. Here we show that a many-body theory based on nonequilibrium Green functions satisfies both criteria. Dynamical information is calculated by a self-consistent theoretical approach, and a novel perspective on nonlinear scattering phenomena results in terms of many-body photon polarization processes which scale with system size.

We consider the example of an optical parametric oscillator (OPO) operating below threshold. This is described below. The semiclassical linearized theory of quantum fluctuations predicts quadrature squeezing of the signal output, which increases as threshold is approached [3,9]. Divergence of the quadrature fluctuations at threshold signifies the breakdown of the theory in the vicinity of the bifurcation point. The threshold photon number in the pump mode, n_{th}, determines the intrin-

sic scale of quantum fluctuations. This is the system-size parameter, and scales approximately in proportion to $(QV/d)^2$, where Q is the quality factor, V the effective volume of the cavity, and d the nonlinearity of the medium [12]. Typically $n_{th} \gg 1$, so that except in the vicinity of threshold, linearization is valid. For small systems, however, reduced thresholds are expected, and many-body photon scattering phenomena which scale with the system size become important. These processes fundamentally alter the nature of the nonequilibrium phase transition predicted by mean-field theory, and the coherence properties of the output. This is also to be expected in the "thresholdless" microcavity lasers [11].

The OPO comprises two discrete optical cavity modes, the subharmonic and pump, which interact due to the presence of the nonlinear intracavity crystal. The nonlinearity enables pump photons with frequency $\omega_2 = 2\omega_1$ to split into two subharmonic photons of frequency ω_1, and vice versa. The pump is driven by a resonant external field, and both modes are damped due to loss through the cavity mirrors. This enables a nonthermal equilibrium to be established. Our model of the OPO below threshold is unitarily equivalent to the master equation of Drummond, McNeil, and Walls [5],

$$\frac{d\rho}{d\tau} = \frac{1}{i\hbar}[H_1 + H_2, \rho] + \sum_{i=1}^{2} \frac{\gamma_i}{\gamma_1}\{2a_i\rho a_i^\dagger - a_i^\dagger a_i\rho - \rho a_i^\dagger a_i\},$$

$$(1)$$

where ρ is the density operator, $\tau = \gamma_1 t$ is time measured in units of the inverse damping rate γ_1^{-1} of the subharmonic mode 1, γ_2 is the damping rate of the pump mode, and the Hamiltonians are defined by

$$H_1 = i\hbar \frac{p}{2}[a_1^{\dagger 2} - a_1^2],$$

$$H_2 = i\hbar \frac{1}{2\sqrt{n_{th}}}[a_1^{\dagger 2}a_2 - a_1^2 a_2^\dagger].$$

$$(2)$$

Here p is a normalized pump parameter, proportional to

the pump laser amplitude, and varies in the range $0 \leq p \leq 1$ between zero pumping and threshold. At threshold the subharmonic undergoes a second order phase transition and attains a nonzero amplitude. Above threshold an additional Hamiltonian term proportional to this amplitude must be included in Eq. (1). The system-size parameter n_{th} corresponds physically to the intracavity pump photon number at threshold. In terms of the usual dimensional parameters of Ref. [5], $n_{th} = (\gamma_1/\kappa)^2$ and $p = \kappa \varepsilon_2 / \gamma_1 \gamma_2$.

In the limit of infinite system size, $n_{th} \rightarrow \infty$, the theory reduces to the usual linearized theory, and predicts perfect quadrature squeezing at threshold [9]. Such an approximation is, however, not uniformly valid in p, in particular at threshold $p = 1$, as is evident from the divergence in fluctuations of the antisqueezed quadrature and the subharmonic photon number. Thus in addition to the intrinsically nonlinear regime when $n_{th} \sim 1$, system-size effects are important even for $n_{th} \gg 1$ in the vicinity of the phase transition where fluctuations are generically large.

In the nonequilibrium Green function technique [13–17] one deals with a matrix Green function propagator in the form

$$i\underline{D}_i(t,t') = \begin{pmatrix} \langle T[a_i^\dagger(t)a_i(t')] \rangle & \langle a_i^\dagger(t)a_i(t') \rangle \\ \langle a_i^\dagger(t)a_i(t') \rangle & \langle \tilde{T}[a_i^\dagger(t)a_i(t')] \rangle \end{pmatrix}$$

$$= i \begin{pmatrix} D_i^{++}(t,t') & D_i^{+-}(t,t') \\ D_i^{-+}(t,t') & D^{--}(t,t') \end{pmatrix}, \quad (3)$$

where T and $\tilde{T}$ are the Dyson time and antitime ordering operators, respectively, and $\langle A,B \rangle \equiv \langle AB \rangle - \langle A \rangle \langle B \rangle$. Keldysh introduced the path ordering operator T_c, which enables the matrix elements to be written in compact form $iD_i^{\zeta\zeta'}(t,t') = \langle T_c[a_i^\dagger(t_\zeta)a_i(t'_{\zeta'})] \rangle$ [14]. In addition to the normal propagator, $\mathcal{D}_i^{\zeta\zeta'}(t,t') = \langle T_c[a_i(t_\zeta)a_i(t'_{\zeta'})] \rangle$ defines the anomalous propagator matrix. These are recognized as the phase dependent correlation functions responsible for squeezing in the semiclassical limit. The output quadrature fluctuation spectrum for the subharmonic mode, normalized to unit shot noise level, is given by

$$V(X_{1\pm},\omega) = 1 + 2\{iD_i^{-+}(\omega) + iD_1^{-+}(-\omega)$$

$$\pm 2\mathrm{Re}[\mathcal{D}_1^{++}(\omega)]\}, \quad (4)$$

where, since we are interested in the steady state, we have used time-translation invariance to introduce the Fourier transforms

$$G_i^{\zeta\zeta'}(\omega) = \int_{-\infty}^{\infty} d\tau \, e^{i\omega\tau} G_i^{\zeta\zeta'}(t+\tau,t), \quad (5)$$

with $G = D$ or $\mathcal{D}$. We note that Eq. (4) corrects an expression given by Zaidi [13].

To proceed we transform to an interaction picture in which the operators evolve according to the cavity reservoir coupling alone, and we denote these with a caret [15]. The Hamiltonian interactions appear in the path-ordered S matrix S_c, e.g.,
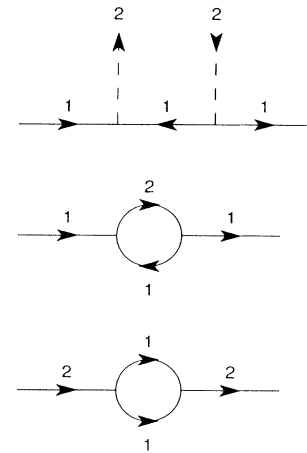
FIG. 1. Diagrammatic representation of fundamental, energy conserving (at each vertex), parametric scattering processes, which are used to renormalize the Green function propagators. The first diagram represents subharmonic photons (directed line) scattering from the mean pump field (dotted line). The second and third diagrams represent photon polarization processes: parametric scattering of subharmonic and pump photons.

$$\langle T_c[a_i^\dagger(t_\zeta)a_i(t'_{\zeta'})] \rangle = \langle T_c[S_c \hat{a}_i^\dagger(t_\zeta)\hat{a}_i(t'_{\zeta'})] \rangle, \quad (6)$$

where

$$S_c = T_c \exp\left[-\frac{i}{\hbar}\int_c [H_1(t) + H_2(t)]dt\right]. \quad (7)$$

The S matrix is expanded in powers of the interaction, and Wick's theorem is used to perform contractions of the multitime correlation functions [16]. The result can be presented in diagrammatic form, and Feynman rules for the parametric interactions deduced [15,17]. The fundamental, parametric scattering processes are illustrated diagrammatically in Fig. 1. All possible scattering events are constructed from these basic diagrams. The renormalized Green functions, ignoring vertex corrections in the limit $1 \ll n_{th} < \infty$, are illustrated in Fig. 2. The corresponding matrix Dyson equations for the subharmonic and pump modes are given by (details will be published elsewhere [18])

$$\tilde{\underline{D}}_1(\omega) = \hat{\underline{D}}_1(\omega) + \hat{\underline{D}}_1(\omega)\underline{\Pi}_1(\omega)\tilde{\underline{D}}_1(\omega),$$

$$\underline{D}_1(\omega) = \tilde{\underline{D}}_1(\omega) + \tilde{\underline{D}}_1(\omega)[-p\underline{\sigma}_3]\underline{\mathcal{D}}_1(\omega),$$

$$\underline{\mathcal{D}}_1(\omega) = \tilde{\underline{D}}_1^T(-\omega)[-p\underline{\sigma}_3]\underline{D}_1(\omega),$$

$$\underline{D}_2(\omega) = \hat{\underline{D}}_2(\omega) + \hat{\underline{D}}_2(\omega)\underline{\Pi}_2(\omega)\underline{D}_2(\omega),$$

$$(8)$$

where $\underline{\sigma}_3 = \mathrm{diag}(1,-1)$ is the third Pauli matrix, and superscript T denotes a real transpose; $\tilde{\underline{D}}_1$ is a partially renormalized Green function for the subharmonic, and $\hat{\underline{D}}_1$ and $\hat{\underline{D}}_2$ are the empty cavity Green functions for the subharmonic and pump, given in the Markov approxima-
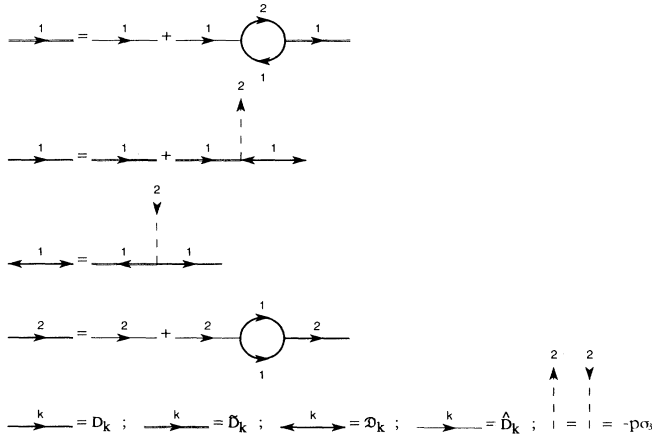
FIG. 2. Diagrammatic representation of the Dyson equations for the propagator matrices. Thin and thick directed lines represent empty-cavity and fully renormalized propagator matrices, respectively, while the anomalous propagator matrix is represented by a two-way directed line. A partially renormalized propagator matrix is denoted by a directed line composed of two thin lines. The mean pump field, given by a broken line, has one free end.

tion by

$$
\hat{\underline{D}}_1(\omega) = \begin{pmatrix} \dfrac{1}{-\omega+i} & \dfrac{-2i}{\omega^2+1} \\ 0 & \dfrac{1}{\omega+i} \end{pmatrix} ,
$$

$$
\hat{\underline{D}}_2(\omega) = \begin{pmatrix} \dfrac{1}{-\omega+i\Gamma} & \dfrac{-2i\Gamma}{\omega^2+\Gamma^2} \\ 0 & \dfrac{1}{\omega+i\Gamma} \end{pmatrix} , \tag{9}
$$

with $\Gamma = \gamma_2/\gamma_1$. The many-body polarization matrices $\underline{\Pi}_i$, represented by the bubble diagrams in Fig. 2, scale with the system-size parameter n_{th}, and have matrix elements

$$
-i\Pi_1^{\alpha\beta}(\omega) = \frac{1}{n_{th}} \frac{\alpha\beta}{2\pi} \int_{-\infty}^{\infty} d\omega' D_1^{\beta\alpha}(-\omega') D_2^{q\beta}(\omega-\omega') ,
$$
$$
-i\Pi_2^{q\beta}(\omega) = \frac{1}{n_{th}} \frac{\alpha\beta}{2\pi} \int_{-\infty}^{\infty} d\omega' D_1^{q\beta}(\omega') D_1^{q\beta}(\omega-\omega') . \tag{10}
$$

We obtain nonperturbative solutions to the Dyson equations (8)–(10) numerically, by self-consistently iterating until convergence is achieved. The main difficulty, i.e., calculation of the polarization parts, is efficiently handled by the use of fast Fourier transforms [18].

To gain some insight into these expressions, first consider the limit $n_{th} \to \infty$, in which the polarization parts vanish, and the partially renormalized propagator $\underline{D}_1$ $\to \underline{\hat{D}}_1$, the empty cavity propagator. Equations (8) then reduce to the linearized quantum theory of the OPO. The coupling between normal and anomalous propagators accounts for the parametric scattering of subharmonic

photons from the mean pump field of amplitude p to infinite order. This is reminiscent of the coupling between normal and anomalous propagators in an interacting Bose gas or superconductor, due to the scattering of noncondensate particles from the condensate mean field [17]. The quantum fluctuations of the pump field do not affect the subharmonic at this level of approximation.

In the nonperturbative regime, with n_{th} finite, the quantum fluctuations of the pump effectively dress the subharmonic empty cavity propagator $\hat{D}_1 \to \bar{D}_1$ as a result of many-body parametric scattering processes from the quantized pump field; these are incorporated in the subharmonic polarization Π_1 [13]. Of course these scattering processes also modify the empty cavity propagation of pump photons, which then reacts back on the subharmonic mode. This backaction is properly accounted for by the polarization Π_2.

Nonperturbative results for the second order coherence $g_1^{(2)}(\tau)$ and intensity fluctuation spectrum $V_I(\omega)$ are also of interest. In many-body theory, these quantities involve the calculation of the polarization propagator—a special case of the two-particle Green function. Normalized to unit shot noise,

$$
V_I(\omega) = 1 + 2\langle n_1 \rangle \int_{-\infty}^{\infty} d\tau [g_1^{(2)}(\tau) - 1] e^{i\omega\tau} , \tag{11}
$$

where $\langle n_1 \rangle$ is the mean subharmonic photon number,

$$
g_1^{(2)}(\tau) = \frac{\langle \hat{T}[a_1^{\dagger}(0)a_1^{\dagger}(\tau)] T[a_1(\tau)a_1(0)] \rangle}{\langle a_1^{\dagger}(0)a_1(0) \rangle^2} , \tag{12}
$$

and the polarization propagator is defined

$$
i^2 \mathcal{P}_1^{-+}(\tau) = \langle T_c [a_1^{\dagger}(0_-)a_1^{\dagger}(\tau_-)a_1(\tau_+)a_1(0_+)] \rangle . \tag{13}
$$

We solve for the polarization propagator diagrammatically using an approximation which excludes any vertex corrections. This is the usual Hartree-Fock approxima-
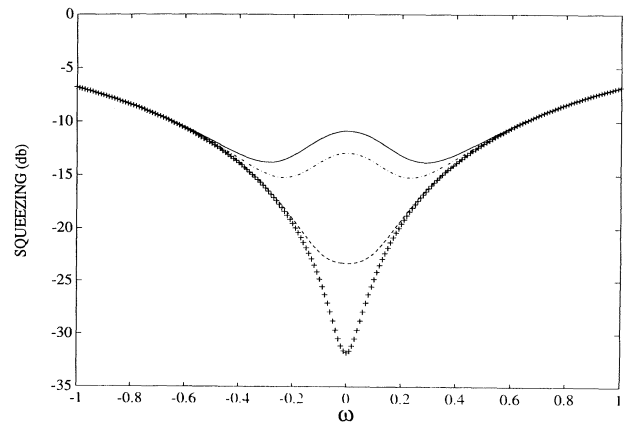
FIG. 3. Spectrum of squeezing at 95% of threshold ($p = 0.95$), $\Gamma = 0.1$, for $n_{th} = 600$ (solid line), 10^3 (dash-dotted line), 10^4 (dashed line), and linearized ($+$).
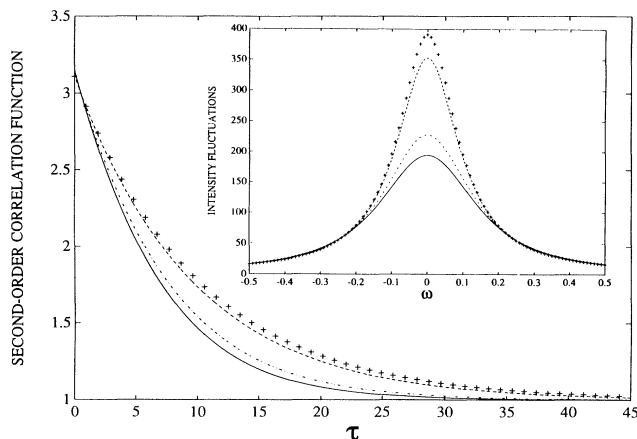
FIG. 4. Second-order correlation function, $g_1^{(2)}(\tau)$, for the same parameters as Fig. 3. Inset shows the corresponding intensity fluctuation spectrum, $V_I(\omega)$, with unit shot noise.

tion for a two-particle Green function, except that here we must renormalize anomalous propagators also. For the OPO system, the lowest class of vertex corrections involves pump mode Green functions proportional to $1/n_{\text{th}}$. Provided n_{th} is not of order unity or smaller, it is reasonable to drop these contributions. In this pseudo Hartree-Fock approximation, the polarization propagator is given by

$$i^2 \mathcal{P}_1^{-+}(\tau) = [\mathcal{D}_1^{++}(\tau)]^2 - [D_1^{-+}(\tau)]^2 + \langle n_1 \rangle^2,$$

where $D_1^{-+}(\tau)$ and $\mathcal{D}_1^{++}(\tau)$ are the fully nonlinear Green functions calculated self-consistently as outlined above.

We remark that the many-body theory agrees with the nonlinear adiabatic theories [4–8] in the limit $\Gamma \gg 1$ for the calculation of single time averages. Dynamical observables are calculated by self-consistent iteration of the Dyson equations (8) until convergence. Figure 3 shows the squeezing spectrum (4) in the nonadiabatic regime, $\Gamma = 0.1$ and $p = 0.95$ (95% of oscillation threshold) for various system sizes, $n_{\text{th}} = 600$, 10^3, 10^4, and ∞. As expected, the squeezing is reduced in the quantum limit. The effects of finite system size embodied in the many-photon polarization processes are thus quantified. Near the bifurcation point system-size scaling is quantitatively important, with a central peak emerging for small enough system size, $n_{\text{th}} = 600$ and 1000. In Fig. 4 we plot the second order coherence and intensity fluctuation spectrum for the same parameter set as Fig. 3. Nonexponential decay of the correlation function is evident for finite system size, as a result of the non-Gaussian fluctuations. The intensity fluctuation spectrum shows that system-size effects substantially suppress the fluctuations near thresh-

old as one expects. Both of these features are understood in terms of the many-body polarization of subharmonic photons by parametric scattering from the pump.

In summary, we have shown that a many-body approach provides a powerful method for the analysis and interpretation of nonlinear quantum dissipative phenomena in quantum optics.

[1] Fluctuations and Sensitivity in Nonequilibrium Systems, edited by W. Horsthemke and D. K. Kondepudi, Springer Proceedings in Physics Vol. 1 (Springer, New York, 1984).

[2] See the special feature editions J. Mod. Opt. 34, No. 6 (1987); J. Opt. Soc. Am. B 4, No. 10 (1987).

[3] L. A. Wu, H. J. Kimble, J. L. Hall, and H. Wu, Phys. Rev. Lett. 57, 2520 (1986); L. A. Wu, Min Xiao, and H. J. Kimble, J. Opt. Soc. Am. B 4, 1465 (1987).

[4] R. Graham, in Quantum Statistics in Optics and Solid-State Physics, edited by G. Hohler, Springer Tracts in Modern Physics Vol. 66 (Springer, New York, 1973), p. 1.

[5] P. D. Drummond, K. J. McNeil, and D. F. Walls, Opt. Acta 28, 211 (1981).

[6] D. F. Walls and G. J. Milburn, in Quantum Optics, Experimental Gravity and Measurement Theory, edited by P. Meystre and M. O. Scully (Plenum, New York, 1983), p. 209.

[7] P. Kinsler and P. D. Drummond, Phys. Rev. Lett. 64, 236 (1990); ibid. Phys. Rev. A 43, 6194 (1991).

[8] M. Wolinsky and H. J. Carmichael, Phys. Rev. Lett. 60, 1836 (1988); F. Kartner, R. Schack, and A. Schenzle, J. Mod. Opt. 39, 917 (1992).

[9] M. J. Collett and D. R. Walls, Phys. Rev. A 32, 2887 (1985).

[10] R. J. Thompson, G. Rempe, and H. J. Kimble, Phys. Rev. Lett. 68, 1132 (1992).

[11] R. E. Slusher, Optics and Photonics News 4, 8 (1993).

[12] P. D. Drummond, K. J. McNeil, and D. F. Walls, Opt. Acta 27, 321 (1980).

[13] H. R. Zaidi, Can. J. Phys. 66, 164 (1988); 66, 854 (1988).

[14] L. V. Keldysh, Zh. Eksp. Teor. Fiz. 47, 1515 (1964) [Sov. Phys. JETP 20, 1018 (1965)].

[15] E. M. Lifshitz and L. P. Pitaevskii, Physical Kinetics, Course of Theoretical Physics Vol. 10 (Pergamon, Oxford, 1981).

[16] G. C. Wick, Phys. Rev. 80, 268 (1950).

[17] A. A. Abrikosov, L. P. Gor'kov, and I. E. Dzyaloshinski, Methods of Quantum Field Theory in Statistical Physics (Dover, New York, 1963).

[18] C. J. Mertens, T. A. B. Kennedy, and S. Swain, Phys. Rev. A 48, 2374 (1993).